

Role of magnetic resonance imaging in evaluation of hydrocephalus

¹Dr. Misba Manzoor Bhat, Senior Resident, Department of Radiodiagnosis.

²Dr. Sadaf Shahzad, Senior Resident, Department Radiodiagnosis.

³Dr. Rajesh Sharma, Professor, Department of Radiodiagnosis.

⁴Dr. Smarth Nathyal, Senior Resident, Department of Radiodiagnosis.

Corresponding Author: Dr. Smarth Nathyal, Senior Resident, Department of Radiodiagnosis.

Citation this Article: Dr. Misba Manzoor Bhat, Dr. Sadaf Shahzad, Dr. Rajesh Sharma, Dr. Smarth Nathyal, “Role of magnetic resonance imaging in evaluation of hydrocephalus”, IJMSIR- November - 2022, Vol – 7, Issue - 6, P. No. 279 – 287.

Type of Publication: Original Research Article

Conflicts of Interest: Nil

Abstract

Background: The advent of imaging of human central nervous system non-invasively has completely changed the diagnostic approach to the pathology of brain. MRI has proved to be the most superior imaging modality in the diagnosis of hydrocephalus and its underlying etiology. PC-MRI and 3D-SPACE are excellent sequences in determining the level of obstruction.

Objective: To characterize the type of hydrocephalus on MRI, to determine the site of obstruction and to evaluate the underlying etiology.

Results: Majority of the subjects (62%) had intraventricular obstructive hydro Cephalus, 32% had extra ventricular obstructive hydro Cephalus, while 6% subjects had hydro Cephalus due to CSF over production. 32% cases had obstruction outside the ventricular system, 30% at 4th ventricular level, 18% at cerebral aqueduct, 10% at 3rd ventricular level and 4% at the level of foramen of monro. Tumors and infections were the most common causes (32% each), followed by aqueduct AI stenosis (10%), IVH (6%), Intraparenchymal hemorrhage with intraventricular extension, Chiari 2,

DWM, Colloid cyst and arachnoid cyst (4% each). Ventricular size was measured using Evan’s index, Frontal horn ratio, Frontal and occipital horn ratio and Bicaudate index. All the indices were increased in the subjects suggesting ventricular dilatation. No significant difference in the indices was noted between various types of hydro Cephalus (p value >0.05), except bicaudate index which was higher in extra ventricular than intraventricular obstructive hydro Cephalus (p value 0.0123).

Conclusions: MRI is an excellent modality to evaluate patients with hydrocephalus and to delineate the type of hydrocephalus, site of obstruction and the underlying etiology and MRI helps in deciding the accurate management of these patients.

Keywords: Hydro Cephalus; MRI, CSF Analysis, Obstruction, Etiology.

Introduction

Hydrocephalus is a complex disorder that can develop for various reasons. Dilatation of the ventricular system may lead to loss of brain cells resulting in a variety of neurological symptoms, stroke, and sometimes even

death due to pressure effect on the brain parenchyma (Algin O et al.,2012). The causes of CSF increase are often obstructive diseases such as cystic lesions, tumors or obstructive membranes (Hing Wala D et al.,2011; Algin O et al., 2013; Hodel J et al.,2013). Rarely, it may be the result of excessive CSF production, which may be due to pathologies at the sites where CSF production takes place. More frequently, it is due to an obstruction in the ventricular system, at or proximal to the fourth ventricular outlet foramina (intraventricular obstructive type) or interrupted CSF absorption or obstruction outside the ventricular system (extra ventricular obstructive type). Earlier, the terms non-communicating and communicating hydrocephalus were used to represent obstruction within or outside the ventricular system (Haacke EM et al.,2009). In young adults and children, obstructive-type hydrocephalus is the most common type (Bonetti MG et al., 2006; Algin O et al.,2013). In some instances, such as meningitis, both absorption and flow may be interrupted, which is defined as complex-type hydrocephalus (Algin O,2010). Although there are several theories regarding the pathophysiology of hydrocephalus, recently the most widely accepted one has been Greitz's hyperdynamic flow theory, which divides hydrocephalus into two main groups, acute and chronic hydrocephalus (Greitz's D, 2004). Acute hydrocephalus is caused by an intraventricular CSF obstruction. Chronic hydrocephalus is further divided into communicating and chronic obstructive hydrocephalus. The theory proposes that chronic hydrocephalus is a result of decreased intracranial capillaries, which causes restricted arterial pulsations, increased capillary pulsations and decreased intracranial compliance (Greitz D,2004).

The advent of imaging of the human central nervous system non-invasively has completely changed the

diagnostic approach to the pathology of brain. During the past few decades, technical advancements have yielded up variety of examinations that produce detailed anatomic or physiologic information without subjecting the patient to a highly invasive or painful procedure. On the basis of ultrasound examination results, hydrocephalus can be diagnosed in most of the infants. However, in older children, where the trans fontanelle ultrasound is impossible, the examination of choice is cross-sectional imaging (CT or MRI). Nowhere is the contribution of non-invasive imaging more appreciated than with MRI and CT which have clearly dominated the field of non-invasive neuro imaging in the diagnosis of hydrocephalus and its causes. Hydrocephalus is not a disease but a dynamic process which proceeds with changes of ventricular system size. Hydrocephalus is characterized by imbalance of cerebrospinal fluid formation and absorption. It is manifested as a dilatation of ventricular system. About 55% of all hydrocephalus cases have congenital origin. A number of different descriptions and radiologic classification schemes for hydrocephalus have been proposed over the years (GreitzD,2004; ReKate HL, 2008; ReKate HL,2009). However, in the past, surgical therapy, irrespective of the classification, consisted of ventricular or lumbar cerebrospinal fluid (CSF) drainage to the right atrium or the peritoneal cavity. Therefore, the demand for imaging was limited to just diagnosis of hydrocephalus. However, the availability of different surgical treatment options necessitates the precise classification of hydrocephalus, in order to be able to select the best treatment modality, avoiding shunt insertion, and to be able to compare results, because our ultimate goal with imaging is to be able to predict the success of treatment before surgery and to expand the indications of neuro endoscopic procedures, and to demonstrate the key issue of level of

obstruction (s). To achieve these goals, imaging modality should provide excellent imaging capability to demonstrate all possible obstructive pathological processes at any level throughout the CSF pathway from the ventricles to the cortical subarachnoid compartment (Rekate HL, 2008; Dincer A et al., 2009).

MRI is not only beneficial in the diagnosis of CSF-related diseases, but also aids in therapy planning and post-surgery follow-up of the patients. The PC-MRI and/or 3D-SPACE methods are relatively simple for evaluating true CSF flow and determining the obstruction level. Also, these techniques provide additional physiological information. The 3D-SPACE technique seems to be the most efficient and rapid for evaluating hydrocephalus. MRI is the single best imaging modality for covering all of the imaging demands, providing one-stop shopping.

Methods

This study was conducted in the Postgraduate Department of Radiodiagnosis, Government Medical College, Jammu. It was a prospective study conducted over a period of one year from November 2020 to October 2021 using “Siemens Magnetom Symphony” 1.5 Tesla Helium cooled super conducting MR scanner.

The study population included patients of hydrocephalus from Department of Medicine and Surgery, GMC Jammu and Department of Pediatrics, SMGS Hospital, Jammu referred to our department for MRI evaluation.

Examination technique and protocol

The imaging was performed using “Siemens Magnetom Symphony” 1.5 Tesla Helium cooled superconducting MR scanner. Dedicated head coil was used for multiplanar imaging of the brain. Counseling of the patient’s attendants regarding the scanning technique was done including the description of the expected duration of the examination and the amount of noise generated

during the scanning. Now, since majority of the patients were infants and young children, who could not stay still for long time therefore, sedation of these patients was important.

The most commonly used sedating agent was Syrup Triclofos (500mg/5 ml). Dosage given was 25-30 mg/kg (up to 1 year), 250-500mg (for 1-5 years of age) and 500-1000 mg (6-12 years). However, when the patient failed to get sedated by the oral drug, then IV sedating drugs were given under the supervision of a pediatric resident. The IV sedating agent used for children was midazolam. Before performing the MR imaging, informed consent was taken from the patient’s attendant regarding the entire procedure (including the sedation and contrast if required).

Detailed history regarding the onset and duration of the symptoms was taken and a brief neurological examination was also performed so that the clinical and imaging findings could be correlated at a later time so as to come to a better diagnosis.

Conventional unenhanced study was performed by applying T1W, T2W and IR sequences in the axial, sagittal and coronal planes.

Apart from these conventional sequences, special sequence such as DWI (Diffusion weighted imaging) and Magnetic Resonance spectroscopy (MRS) were also applied, wherever necessary.

Contrast was administered wherever necessary. In such cases, post contrast T1W sequence was applied in axial, coronal and sagittal plane. The contrast agent used was gadolinium-DTPA.

The dose of the contrast given was 0.1 mmol/ kg body weight.

The acquisition parameters that were used are as under-

- T1-weighted: TR -195 Ms, TE - 4.8 Ms, BW -150, slice thickness - 5 mm.

- T2 -weighted: TR - 3500 Ms, TE - 92 Ms, BW-191, slicethickness-5 mm
- IR: TR - 9000 Ms, TE - 113 Ms, BW- 190, slice thickness- 5 mm
- DWI: TR - 3500 Ms , TE - 106 Ms, BW- 985, slice thickness-5 mm
- SPC: TR- 1200, TE- 266
- MP-RAGE: TR-2200, TE- 4.4
- PC: TR-81.4, TE- 10.6
- SWI: TR-49, TE-40

The MR image morphology on conventional sequences and additional (above specified sequences) and post contrast sequences (if any) were then evaluated under the supervision of my guide and a differential diagnosis was thus formulated.

Results

Majority of subjects were infants (28%) and Children of age group 1-10years (24%), followed by adults and adolescents (Table 1).

Table 1: Age wise distribution of subjects in the study (n=50)

Age	Count	%
<1 year	14	28%
1-10 years	12	24%
11-20 years	05	10%
21-30 years	07	14%
31-40 years	05	10%
41-50 years	07	14%

Majority of subjects had headache (30%), fever (22%), balance abnormalities (20%), seizures (18%), vomiting (12%), followed by other symptoms (Table 2).

Table 2: Clinical symptoms in subjects

Symptoms	Count	%
Headache	15	30%
Fever	11	22%
Balance abnormalities	10	20%
Seizures	09	18%
Vomiting	06	12%
Refusing feeds	03	6%
Visual defects	03	6%
Syncope	02	4%
Confusion	02	4%
Drowsiness	02	4%
Hearing defects	01	2%
Nystagmus	01	2%
Hemiparesis	01	2%

CSF Analysis was done in 11 out of 50 subjects out of whom 6 had tubercular meningitis, 4 had bacterial meningitis and 1 had NCC (Table 3).

Table 3: CSF analysis in subjects.

CSF Analysis	Count	%
Not done	39	78%
Tubercular meningitis	06	12%
Bacterial meningitis	04	8%
NCC (anti cyst I cercal antibodies)	01	2%

Lateral ventricles were dilated in all subjects (100%), third ventricle was dilated in 80%, normal in 18% and obliterated in 2%, while fourth ventricle was dilated in 40%, normal in 42% and obliterated in 18% cases (Table 4).

Table 4: MRI findings in subjects

Site	Condition	Count	%
Lateral Ventricles	Dilated	50	100%
	Not dilated	0	0%
3 rd Ventricle	Dilated	40	80%
	Not dilated	09	18%
	Obliterated	01	2%
4 th Ventricle	Dilated	20	40%
	Not Dilated	21	42%
	Obliterated	09	18%
Periventricular ooze	Present	38	76%
	Absent	12	24%

62% of the subjects had intraventricular obstructive hydrocephalus, 32% had extra ventricular obstructive hydrocephalus, while 6% subjects had hydro Cephalus due to CSF overproduction (Fig 1).

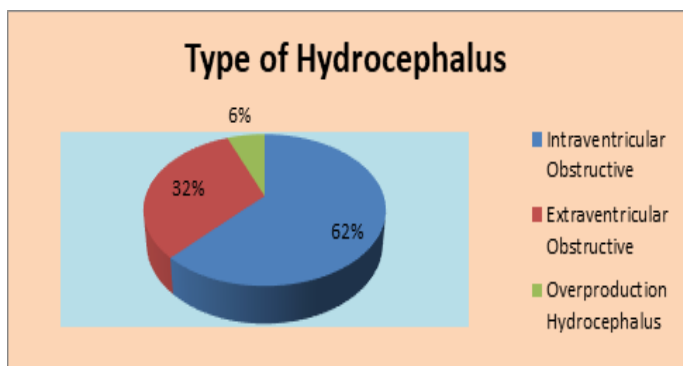


Fig 1.

In the study, 32% cases had obstruction outside the ventricular system, 30% at 4th ventricular level, 18% at cerebral aqueduct, 10% at 3rd ventricular level and 4% at the level of foramen of monro (Fig 2).

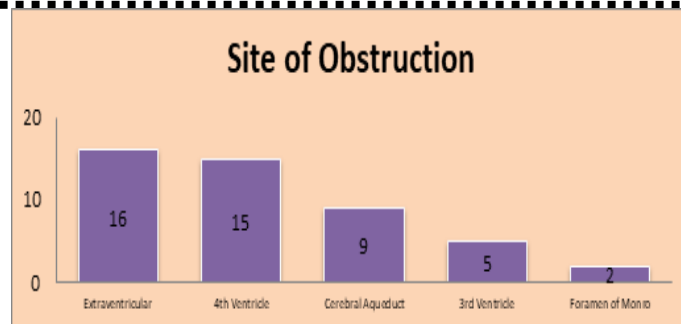


Fig 2

No significant difference between Evan’s index, FHR and FOHR was noted between intra and extra ventricular obstructive hydrocephalus (p value >0.05), whereas, bicaudate index was higher in EVOH than IVOH (p value 0.0123) (Fog 3).

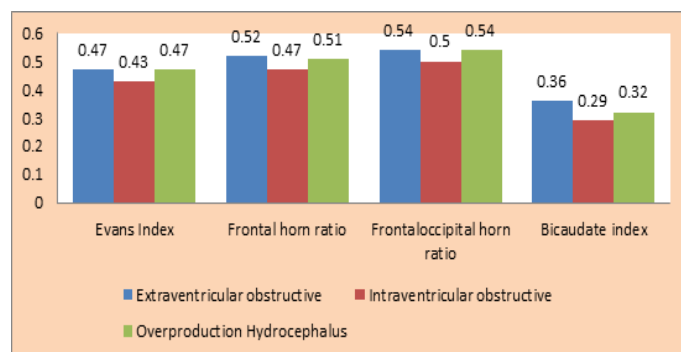


Fig 3.

The underlying etiology was tumors and infections in majority of subjects (32% each), followed by aqueduct al stenosis (10%), IVH (6%), Intra parenchymal hemorrhage with intra ventricular extension, chiari 2, DWM, Colloid cyst and arachnoid cyst (4% each) (Fig 4).

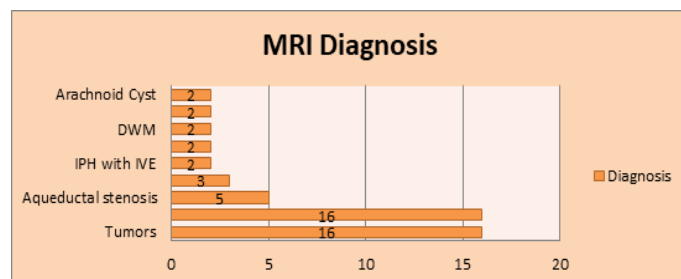
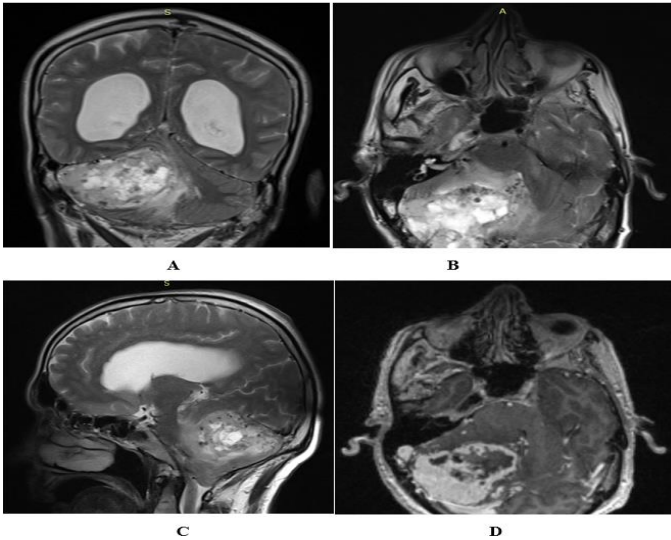


Fig 4.

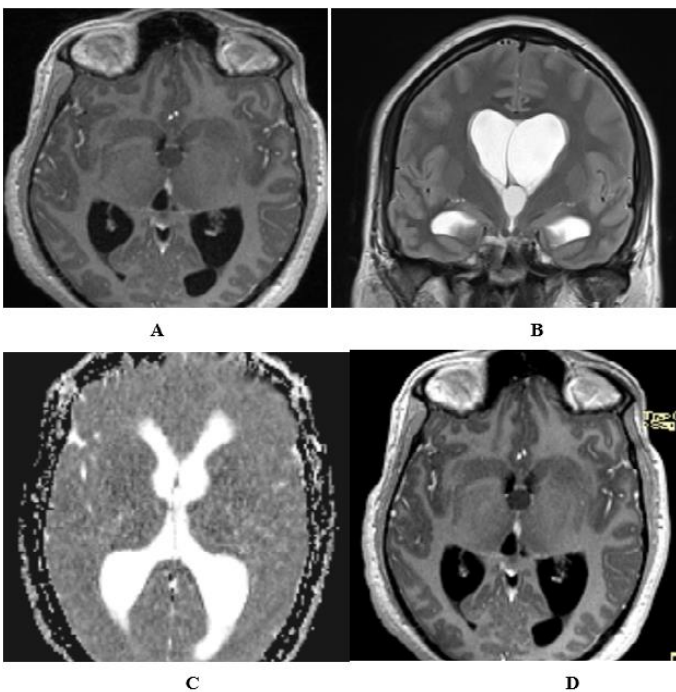
Case 1: cerebellar hemangioblastoma



• Coronal (Fig. A), Axial (Fig. B) and Sagittal (Fig. C) T2W images showing a heterogeneously hyperintense right cerebellar mass with internal flow voids, causing compression on 4th ventricle with resultant supratentorial hydrocephalus.

• Axial post contrast image (Fig. D) shows intense enhancement of solid component.

Case 2: colloid cyst at roof of 3rd ventricle (FoM)

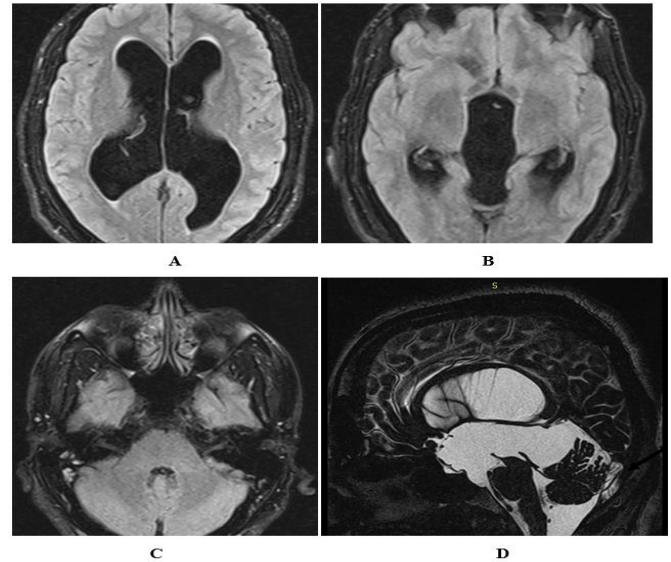


• A well-defined lesion noted at the roof of third ventricle (Foramen of Monro) appearing isointense on

T1W (Fig. A) and hyperintense on T2W images (Fig. B) with no diffusion restriction (Fig. C). Resultant dilatation of lateral ventricles noted.

• Axial postcontrast T1W image (Fig. D) shows minimal rim enhancement.

Case 3: aqueductal stenosis due to aqueductal web



• Axial FLAIR images showing dilated lateral ventricles (Fig. A) and 3rd ventricle (Fig. B) with normal sized 4th ventricle (Fig. C).

• Sagittal T2 SPC image (Fig. D) shows narrowing at the level of cerebral aqueduct with low signal intensity band (arrow) across the cerebral aqueduct.

Discussion

Diagnosis of hydrocephalus has improved considerably over the years with the advent of various imaging modalities. In earlier times, it was a challenge to prove the fact that excessive fluid inside the head was the cause of hydrocephalus and its effects. Though plain X-rays were indicative, they were not necessarily confirmatory. Air and contrast ventriculography were the key diagnostic investigations. The introduction of computed tomography (CT) and magnetic resonance imaging (MRI) has rapidly advanced the detection and treatment. Management of hydrocephalus in the form of

ventriculoperitoneal (VP) shunts has risen in many centers across the country.

Hydrocephalus is a common clinical problem seen in pediatric neurosurgical practice. Hydrocephalus involves dilatation of the cerebral ventricular system with corresponding compressive effects on the parenchyma. Congenital, acquired, infective and secondary hydrocephalus have different clinical features and different modalities of treatments. Obstruction at any point along the CSF pathway may result in hydrocephalus.

In our study, majority of subjects were infants (28%) and Children of age group 1-10years (24%), followed by adults and adolescents, consistent with findings of Isaacs A Met al., (2018) and Khan MU et al., (2018).

In our study, children under 2 years with symptoms of hydrocephalus had large head circumference, bulging anterior fontanelle and setting sun sign of the eyes consistent with findings of Losowska KD et al., (2007). Older children and adults presented with classical symptom consisting of raised ICP, headache, and vomiting, as explained by Venkataraman a NK et al., (2011).

In a study done by Foss-Skiftesvik Jet al., (2013), mean Evan's index was >0.3 in all types of hydrocephalus and it was higher in cerebral pathologies as compared to extra ventricular pathologies. In our study too, Evan's index was >0.3 in all cases. However, in our study, no significant difference in Evan's index between intra and extra ventricular types of hydrocephalus was noted (p value >0.05).

The mean Bicaudate Index in our study was 0.29 in IVOH, 0.36 in EVOH and 0.32 in OPH. All these values are higher than the normal upper limit of Bicaudate index which was found to be 0.21. (Foss-Skiftesvik J et al., 2013)

In our study, out of 50 cases, 31(62%) had intraventricular obstructive hydrocephalus, 16(32%) had extra ventricular obstructive and 3 (6%) had overproduction type of hydrocephalus. Among the obstructive type, 32% cases had obstruction outside the ventricular system, 30% at 4th ventricular level, 18% at cerebral aqueduct, 10% at 3rd ventricular level and 4% at the level of foramen of monro. These findings are consistent with the studies by Algin O et al., (2012) suggested that in childhood, obstructive hydrocephalus is the most common type of hydrocephalus and ReKate HL et al., (2016) suggested that the most common type of hydrocephalus is obstructive.

Martis DR and Rasquinha DS (2014) studied 80 patients from Mangalore with hydrocephalus. The study showed TB meningitis as the major cause of hydrocephalus accounting 26(32.5%) of the cases. The next two important causes were tumors 20(25%) and intracranial haemorrhage 16(20%). These findings are consistent with our study where meningitis and tumors were the most common causes. In our study the third commonest causes were aqueductal stenosis and intracranial hemorrhage (10% each).

In a study done by Kingsely D and Kendall BE (1978) on a series of 109 cases of hydrocephalus, tumors were the commonest cause of hydrocephalus (56 cases -51%) followed by communicating hydrocephalus (20 cases-18%), aqueduct stenosis (17 cases-16%) and posterior fossa cysts (16 cases-15%).

Garg R Ket al., (2016) did a retrospective review of CT findings in 289 patients with tuberculous meningitis, which revealed that 254 (88%) patients had some form of imaging abnormality. The common changes included hydrocephalus (204 patients), parenchymal enhancement (62 patients), contrast enhancement of basal cisterns (49 patients), cerebral infarcts and focal or diffuse brain

edema (39 patients), and one or more cerebral tuberculomas (14 patients). These observations are also consistent with our study. However, cerebral infarcts were not noted in any of our subjects.

Conclusion

Our study suggested that, MRI is an excellent modality to evaluate patients with hydrocephalus and to delineate the type of hydrocephalus, site of obstruction and the underlying etiology and MRI helps in deciding the accurate management of these patients.

References

1. Abdelhameed AM, Darweesh EAF, Bed air MH. Role of MRI CSF Flowmetry in Evaluation of Hydrocephalus in Pediatric patients. The Egyptian Journal of Hospital Medicine 2017;68(2):1291-96.
2. Alford EN, Rotman LE, Shank CD, Agee BS, Market JM. Independent validation of the colloid cyst risk score to predict symptoms and hydrocephalus in patients with colloid cysts of the third ventricle. World neurosurgery 2020;134:e747-53.
3. Algin O, Hakyemez B, Parlak M. Phase contrast MRI and 3D-CISS versus contrast-enhanced MR Cisternography in the evaluation of the aqueductal stenosis. Neuroradiology 2010 52:99-108.
4. Algin O, Ozmen E, Karaoglanoglu M. The role of MRI in Pediatric obstructive hydrocephalus: An update. Journal of Pediatric Neuroradiology 2012;2:71-80.
5. Algin O, Turk bey B Intrathecal gadolinium-enhanced MR cisternography: A comprehensive review. AJNR Am J Neuro Radiol 2013;34(1):14-22.
6. Algin O, Turk bey B. Evaluation of aqueductal stenosis by three-dimensional sampling perfection with application optimized contrasts using different flip-angle evolutions (3D-SPACE) sequence: Preliminary results with 3 Tesla MRI. AJNR Am J Neuro Radiol 2012; 33: 740 -46.

7. Algin O. Role of complex hydro Cephalus in unsuccessful endoscopic third ventriculostomy. Child's Nerv Syst 2010; 26 (1):3-4.
8. Anania P, Battaglini D, Balestri no A, D'Andrea A, Prior A, Ceraudo M et al. The role of external ventricular drainage for the management of posterior cranial fossa tumours: a systematic review. Neurosurgical Review 2021;44(3):1243-53.
9. Barbosa JH, Santos AC, Salmon CE. Susceptibility weighted imaging: Differentiating between calcification and hemosiderin. Radiol Bras 2015;48:93-100.
10. BELL JE, Gordon A, Maloney AF. The association of hydrocephalus and Arnold-chiari malformation with spina bifida in the fetus. Neuro pathology and Applied Neuro biology 1980; 6 (1): 29-39.
11. Berg strand G, Bergstrom M, Nor dell B, Stahlberg F, Ericsson A, Hemmings son A et al. Cardiac gated MR imaging of cerebrospinal fluid flow. J Compute Assist Tomogr 1985;9:1003-1006.
12. Bonetti MG, Sc arabino T. Rosi R, Ceddia A, Sal Volini U. Intracranial hypertension. In: SC arabino T, Sal Volini U, Jinkins JR, editors. Emergency neuroradiology. Springer: Berlin Heidelberg 2006;195-237.
13. Bradley WG, Kortman KE, Burgoyne B Flowing cerebrospinal fluid in normal and hydrocephalic states: appearance on MR images. Radiology 1986;159:611-16.
14. Bradley WG, White more AR, Kortman KE, Watanabe AS, Homyak M, Teresi LM et al. Marked cerebrospinal fluid void: indicator of successful shunt in patients with suspected normal-pressure hydrocephalus. Radiology 1991;178:459-66.
15. Cinalli G, Spennato P, Nastro A, Aliberti F, Trischitta V, Ruggiero C et al. Hydrocephalus in aqueductal stenosis. Childs Nerv Syst 2011; 27 (10): 1621 -42.

16. Dandy W. Internal hydrocephalus, an experimental, pathological and clinical study. *Am J Dis Child* 1914; 8: 406 -82.
17. Dandy WE, Black fan KD. Internal hydrocephalus, an experimental, clinical, and pathological study. *Am J Dis Child* 1917;424-43.
18. Desai SB. SWI, a new MRI sequence-how useful it is? *Indian J Radiol Imaging* 2006;16:13-14.
19. Dias MS, Mc Lone DG. Hydrocephalus in the child with dysraphism. *Neuro surgery clinics of North America* 1993; 4(4): 715-26.
20. Dincer A, Kohan S, Ozek MM. Is all “communicating” hydro Cephalus really communicating? Prospective study on the value of 3D-constructive interference in steady state sequence at3 T. *AJNR Am J Neuro Radiol* 2009; 30: 1898 -1906.